13th World Conference on Earthquake Engineering
Vancouver, B.C., Canada
August 1-6, 2004
Paper No. 2420

ANALYSIS OF STEEL PLATE SHEAR WALLS USING EXPLICIT FINITE ELEMENT METHOD

M. R. Behbahanifard[1], G. Y. Grondin[2], and A. E. Elwi[2]
Department of Civil and Environmental Engineering, University of Alberta,
Edmonton, Alberta, T6G 2G7, Canada

SUMMARY

The finite element analysis of unstiffened steel plate shear walls (SPSWs) has been implemented to date with only limited success. Because of local instabilities and snap-through buckling of infill plates, commonly used solution techniques fail to converge to the equilibrium path as cyclic buckling takes place in the plate. Lack of convergence is a major problem in finite element analysis of these systems especially when geometric nonlinearities are included in the model [1, 2].

A finite element model based on explicit dynamic formulation was recently developed for the analysis of unstiffened SPSWs. Shell elements were used to model all components of the shear wall. Material and geometric nonlinearities, and initial imperfections in the infill plates were included in the model. A kinematic hardening material model was implemented in the analysis in order to simulate the Bauschinger effect in the cyclic analysis of the system. A special loading procedure was developed to implement a displacement control analysis. Quasi-static condition was simulated by controlling the kinetic energy of the system.

This paper presents the procedure adopted to analyze SPSWs under monotonic and cyclic loading. It validates the finite element model by comparing the predicted behaviour with the results of a large-scale three-storey SPSW test.

INTRODUCTION

Experimental and analytical investigations have shown that unstiffened steel plate shear walls are effective and economical lateral load resisting systems, especially in regions of high seismicity [1, 2, 3]. The system consists of infill steel plates connected to the boundary beams and columns over the full height of the framed bay. For a thin panel, the shear buckling strength is low and, as a result, the shear

[1] Post Doctoral Fellow, Dept. of Civil & Environmental Engineering, U. of Alberta, Edmonton, AB, Canada
[2] Professor, Dept. of Civil & Environmental Engineering, U. of Alberta, Edmonton, AB, Canada

resistance depends on the ability of the infill plate to develop a tension field. The boundary members must have sufficient flexural stiffness to anchor the tension field.

Clause 27.8 of the latest edition of the Canadian standard on Limit States Design of Steel Structures [4] provides guidelines for the analysis and design of thin unstiffened steel plate shear walls. The analysis method proposed in Clause 27.8 is based on the strip model developed by Thorburn *et al.* [5]. Although the model predicts the capacity of the system reasonably well, it fails to predict the stiffness accurately in most of the cases [3]. Accurate prediction of stiffness is of paramount importance in drift calculations of high-rise buildings. To provide improved design guidelines more research is needed in areas that are still unknown. For example, it is necessary to quantify the effects of infill panel aspect ratio and the stiffness ratio of the infill plate to that of beams and columns. Because of the expense involved in an experimental program to investigate these parameters, an analytical tool that can accurately predict the monotonic and cyclic behaviour of thin unstiffened steel plate shear walls is needed for a comprehensive parametric study.

Despite the recent research progress on this system, mainly due to small and large-scale testing programs, and the attention from the structural engineering community, to date, relatively few structures that use this system have been constructed in North America. The lack of a reliable and effective analytical tool is likely one of the barriers for wide application of this system. The following presents a procedure that has been implemented successfully to predict both the strength and behaviour of SPSWs under monotonic and cyclic loading.

CONVERGENCE PROBLEM IN A STATIC IMPLICIT METHOD

Most large-scale tests on steel plate shear walls have been conducted under quasi-static loading conditions. The response of a nonlinear system should be obtained incrementally. In a static condition, the equilibrium state at the end of a load increment at time $t + \Delta t$ can be written as:

$$\underline{R}_{t+\Delta t} - \underline{F}_{t+\Delta t} = 0 \tag{1}$$

where $\underline{R}_{t+\Delta t}$ are the external forces and $\underline{F}_{t+\Delta t}$ are the internal forces, equivalent to the element stresses. Since $\underline{F}_{t+\Delta t}$ depends on the history of the nodal point displacements, it is necessary to adopt an iterative process to solve the above equation.

The common solution technique for solving the above nonlinear equation is based on Newton-Raphson (or modified Newton-Raphson) iterative method [6]. In a load control analysis, the solution seeks equilibrium through a horizontal path at a constant load vector of $\underline{R}_{t+\Delta t}$. In a displacement control analysis, which is required for tracing the behaviour of a system after a limit point, both the load level and the displacements are treated as unknowns [7]. The basic algorithm remains the Newton-Raphson iteration, but the search for equilibrium is based on an iterative path perpendicular to the tangent at previously converged point. Because of the sudden out-of-plane deformation of infill plates when the infill plate buckles, usually convergence of the analysis cannot be achieved within the tolerance required for accurate results, or requires a very small time increment. An earlier attempt to analyze a three-storey SPSW under monotonic loading required an increment size less than 10^{-5} second (the static analysis conducted in one second virtual time scale) in order to obtain convergence [8]. Because of the poor performance of the implicit finite element method, the explicit dynamic method was adopted as a tool for the analysis of steel plate shear wall systems.

EXPLICIT FINITE ELEMENT METHOD

The explicit dynamic procedure can be used as an effective tool for solving a wide variety of nonlinear solids and structural mechanics problems. Originally it was developed to analyse high-speed dynamic events that are extremely expensive to analyse using implicit methods [9]. With proper control of the kinetic energy, the explicit approach can be used for quasi-static problems that experience severe convergence difficulties in implicit analysis methods.

Formulation of the dynamic explicit finite element method

The governing equilibrium equations of a body in a dynamic state can be obtained using the principle of virtual work. According to this principle, a body is in a state of static or dynamic equilibrium when the total internal virtual work is equal to the total external virtual work when the body is subjected to a virtual displacement. By neglecting the effect of viscous damping the dynamic force balance, in matrix form, can be obtained as:

$$\underline{M}\underline{\ddot{U}} = \underline{R} - \underline{F} \tag{2}$$

Where $\underline{M}$ is the consistent mass matrix, $\underline{\ddot{U}}$ is the nodal acceleration vector, $\underline{R}$ and $\underline{F}$ are external and internal force vectors, respectively, as defined in equation 1. If a lumped mass matrix is used in lieu of a consistent mass matrix, equation (2) can be decoupled and the dynamic balance equation can be written separately for each node. This is an important step in the dynamic explicit formulation since by doing so the time integration procedure can be carried out quite effectively explicitly.

Computational procedure in dynamic explicit method

Using the central difference method, which is the most commonly used time integration procedure, equilibrium of the system is considered at time t in order to calculate the kinematic conditions at time $t + \Delta t$ (the next increment). Because the explicit method uses a lumped mass matrix, the solution of the acceleration is trivial since no simultaneous equations need to be solved:

$$\underline{\ddot{U}}_t = (\underline{M})^{-1}.(\underline{R}_t - \underline{F}_t) \tag{3}$$

As a result, the acceleration of any node is determined completely by its nodal mass and the net force acting on the node, making the nodal calculation very inexpensive. Using central difference method the accelerations are integrated over time to obtain the change in velocity, assuming a constant acceleration. The change in velocity is added to the velocity from the middle of the previous increment to determine the velocity at the middle of the current time increment:

$$\underline{\dot{U}}_{(t+\frac{\Delta t}{2})} = \underline{\dot{U}}_{(t-\frac{\Delta t}{2})} + \left(\frac{\Delta t_{(t+\Delta t)} + \Delta t_t}{2}\right).\underline{\ddot{U}}_t \tag{4}$$

The velocities are then integrated over time and added to the displacements at the beginning of the increment to determine the displacements at the end of the increment as follows:

$$\underline{U}_{(t+\Delta t)} = \underline{U}_t + \Delta t_{(t+\Delta t)}.\underline{\dot{U}}_{(t+\frac{\Delta t}{2})} \tag{5}$$

Therefore, by satisfying dynamic equilibrium at the beginning of the increment, the velocities and the displacements are obtained at the middle and the end of the increment, respectively.

Stability limit of a dynamic explicit method

Since the central difference method is a conditionally stable algorithm [6], the maximum time increment should be less that a stability limit in order to keep the error bounded. The stability limit is defined in terms of the highest frequency of the system, $\omega_{\max}$. In the absence of damping, the stability limit is defined as:

$$\Delta t_{stable} = \frac{2}{\omega_{\max}} \tag{6}$$

Since calculation of the actual highest frequency of a model can be very time consuming, especially in large models, a simple estimate, obtained from the individual elements in the model, that is feasible and conservative, is usually used [10]. The element–by–element method tends to overestimate the highest frequency of the system, which results in a smaller time increment. The highest frequency of an element is associated with the dilatational mode, and the critical time increment is given by:

$$\Delta t_{stable} = \frac{L_e}{C_d} \tag{7}$$

where, L_e is the smallest characteristic length of the element and C_d is the dilatational wave speed of the material defined as:

$$C_d = \sqrt{\frac{E}{\rho}} \tag{8}$$

where, E is the modulus of elasticity and ρ is the density of the material. Examination of these equations reveals that a conservative value for critical time increment is the time that a dilatational wave passes across the smallest characteristic element length.

Two main parameters can change the critical time increment and, as a result, can change the required computational time for an explicit analysis. These are the material properties and size of the finite element mesh. The dilatational wave speed depends on the stiffness and the density of the material. The stiffer the material the higher the wave speed, resulting in a smaller stable time increment. On the other hand, a higher material density results in a reduction of the wave speed and an increase in the critical time increment. For a specific material the wave speed is constant in the linear portion of the analysis since the modulus of elasticity is constant and, therefore, the critical time depends only on the smallest element size in the finite element mesh. In the nonlinear range, however, the modulus of elasticity decreases, which reduces the wave speed and increases the critical time increment. Since the critical time increment is approximately proportional to the shortest element dimension, it is recommended that the element size be kept as large as possible as long as the accuracy of analysis is acceptable.

Simulation of a quasi-static analysis with the dynamic explicit method

Almost all tests on unstiffened steel plate shear walls available in the literature have been conducted under quasi-static loading condition. However, the explicit finite element method is based on a dynamic formulation in which the inertial forces resulting from the acceleration and mass of the system play an important role. As a result, applying the explicit dynamic procedure to a quasi-static problem requires some special considerations. The main goal is to simulate the analysis in the shortest period of time in which the inertial forces remain insignificant. The speed of an analysis often can be increased substantially without significantly reducing the accuracy of quasi-static solutions. However, if the speed of an analysis increases to a point where the inertial forces dominate, the solution tends to localize and the results will be quite different from the quasi-static solution.

For accuracy and efficiency of a quasi-static analysis, loads should be applied as smoothly as possible such that the accelerations change only a small amount from one increment to the next increment. If the acceleration is smooth, it results in a smooth velocity and displacement. ABAQUS/Explicit [10] has a simple built-in type of amplitude, called SMOOTH STEP, which automatically creates the smoothest possible loading amplitude between two points. Using this option, each of the data pairs will be connected with curves whose first and second derivatives are smooth and whose slopes are zero at each data point

In a quasi-static analysis the slowest mode of the structure dominates the response. As a result, by calculating the frequency and period of the slowest mode of the system, a lower bound time period for doing a quasi-static simulation can be obtained. In most structural problems a loading duration corresponding to 10 times the period of the slowest mode is recommended in order to make sure that a solution is quasi-static [10].

In a quasi-static simulation, the kinetic energy of the deforming material should not exceed a small fraction (typically 5% to 10%) of its internal energy during most of the simulation [10]. In addition, a smooth loading history should produce smooth response and as a result the kinetic energy history itself should be smooth.

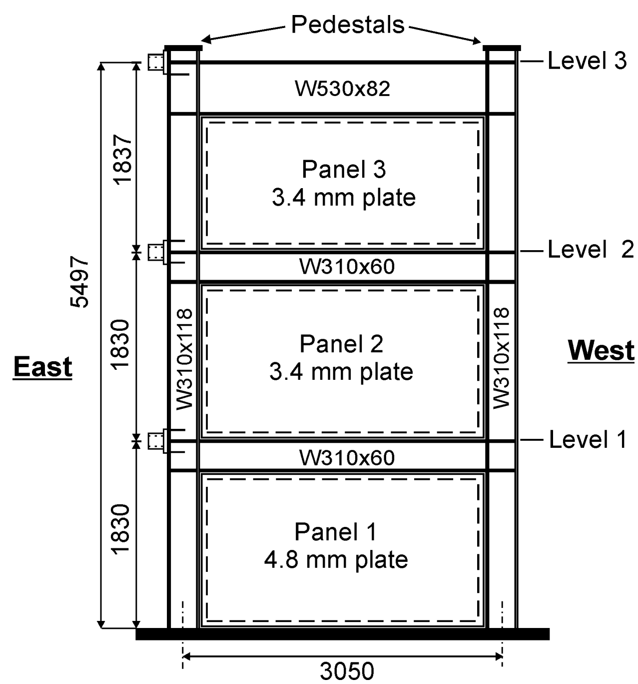

Fig. 1 : Schematic of a 3-storey steel plate shear wall

FINITE ELEMENT ANALYSIS OF LARGE-SCALE THREE-STOREY SPSW

A test on a large-scale three-storey steel plate shear wall was conducted at the University of Alberta [8]. The test specimen consisted of the undamaged upper three storeys of a four-storey SPSW tested by Driver *et al.* [3]. A schematic of the test specimen is shown in Fig.1. The columns consist of W310x118 sections spaced at 3050 mm, and the beams are W310x60 sections at levels 1 and 2 and W530x82 at the top. The overall height of the specimen is 5497 mm with a typical storey height of 1830 mm. The specimen was tested under a combination of constant gravity load and cyclic lateral load under quasi-static condition. Equal lateral loads were applied at each beam level and were cycled according to the guideline proposed by ATC-24 [11] in order to simulate a severe earthquake condition.

Details of the specimen and the test results are presented in reference [8]. The monotonic and cyclic behaviour of the three-storey SPSW specimen were simulated with ABAQUS/Explicit [10] and the results of the analysis are compared with the test results in the following.

Description of finite element model

Element selection

In order to capture local buckling of beam and column flanges, all components of the steel plate shear wall were discretized with shell elements. The "S4R" shell element was selected from the ABAQUS library of elements. This element is a general-purpose 4-node doubly curved shell element with reduced integration and is based on an updated Lagrangian formulation. The element accounts for finite (large) membrane strains and arbitrary large rotations and can be used to model the behaviour of both thin and thick shells. Each node has six degrees of freedom, namely, three translations (u_x, u_y, u_z) and three rotations ($\theta_x, \theta_y, \theta_z$) defined in a global coordinate system.

To prevent the occurrence of hourglass modes, all the concentrated loads and boundary conditions were distributed on a number of nodes; typically 15 nodes for concentrated loads and 5 nodes for lateral bracing points. A mesh of 15 by 10 elements (15 elements over the width of the shear wall) was used to model the infill plates. Beam and column cross-sections were discretized using 12 shell elements and the length of the elements was selected to match the mesh size in the infill plates. Five integration points through the thickness of the shell elements were used in monotonic loading of shear wall and nine integration points were used in more complex cyclic loading.

Geometry and initial imperfections

Measurements of as-built dimensions were used in the finite element model. The fish plate connection tabs, which were used for connection of infill plates to the inside flanges of boundary members in the test specimen, were not considered in the finite element model since they are not expected to affect the overall behaviour of the SPSW. The imperfections can be categorised as camber and sweep of beams and columns and out–of–flatness of the plate. The camber and sweep of the beams and columns and the columns out–of–plumb were considered small and were neglected in the formulation of the finite element model.

The previous test on a four-storey steel plate shear wall [3] from which this three-storey SPSW was obtained had introduced a pattern of residual buckles in the infill plate at the first level, which were consistent with the orientation of the tension field at the time of failure. The maximum value of the out–of–plane initial imperfections was measured to be 39 mm in the first panel. Measured out–of–plane deformations in the first panel were mapped onto the finite element mesh in order to introduce these initial imperfections in model. For the second and third panels, the infill plate was taken to have an initial imperfection pattern corresponding to the buckling mode of the shear wall loaded in the same way as in the test. The peak amplitude for the second and third panels out–of–plane deformations was set at 10 mm.

Boundary conditions

All the nodes at the base of the steel plate shear wall model were fixed to simulate the rigid boundary condition at the base of the shear wall. In order to simulate the out-of-plane bracing provided in the physical test, the out-of-plane displacements at both ends of the beam at all three levels were restrained. In order to prevent local distortions at the brace points, five nodes were restrained at each brace point.

In the physical test the horizontal loads at each floor level and also the gravity loads at the top of each column were applied through thick bearing plates welded to the test specimen. To simulate this effect at all loading points, a rigid body surface was provided by connecting the nodes under the bearing plates to a reference node with rigid links.

Material properties

The constitutive relationship in the analysis is based on stress versus strain responses obtained from tension coupon tests of different parts of the steel plate shear wall. Since it was not possible to conduct material tests for the three-storey specimen, the results of the tension tests on the material used in the fabrication of the Driver *et al.* [3] test specimen, from which the current specimen was obtained, were used. These material properties do not reflect any of the changes in material properties that took place as a result of the plastic deformations during the four-storey shear wall test and, therefore, it has some impact on the results. The steel used in all parts of the shear wall exhibited the classical stress versus strain behaviour of hot rolled ductile steel with a well-defined yield plateau. The engineering stress vs. strain curves were changed to true stress (Cauchy stress) and logarithmic strain for use in the finite element model.

A simple rate independent constitutive behaviour that is identical in tension and compression was used. An isotropic hardening model was used for the pushover analysis. Although ABAQUS/Explicit is intended for dynamic, hence cyclic, analysis, it does not have a kinematic hardening model. However, it allows the user to implement a material model through a user subroutine. A kinematic material model suitable for analysis of a shell element was therefore prepared and used for cyclic load analysis of steel plate shear wall.

Technique for conducting a displacement control analysis

Because of the flat load versus displacement behaviour displayed by the test specimen at large deformations, a displacement control approach is preferred for the analysis so that the loading process can be better controlled. In addition, a load control approach will result in an unstable dynamic solution when the applied load exceeds the load carrying capacity of the shear wall. The need for a displacement control strategy is more vital in a cyclic analysis. A typical loading procedure for a cyclic test of a SPSW consists of selecting a deformation control parameter such as the inter-storey drift, and to control the magnitude of this parameter during the test.

The available control option in ABAQUS/Explicit consists of applying displacement, velocity and/or acceleration histories to one or more nodes separately. These nodes are treated as boundary nodes and the required force at each node to reach a specific displacement (velocity and/or acceleration) is obtained from equilibrium.

During cyclic loading of the three-storey steel plate shear wall, the gravity loads remained constant and the cyclic loads were equal horizontal loads applied at each level. In order to implement a displacement control type analysis, the distributing beam system shown in Fig. 2 was used as a loading frame. The loading frame consists of a system of rigid beam elements that are connected to the shear wall at beam levels in order to transfer horizontal forces only. The geometry and the connections are defined in such a way that any loads applied at node B7 on loading frame is transferred equally to each level of the shear wall. For stability, out–of–plane displacement and

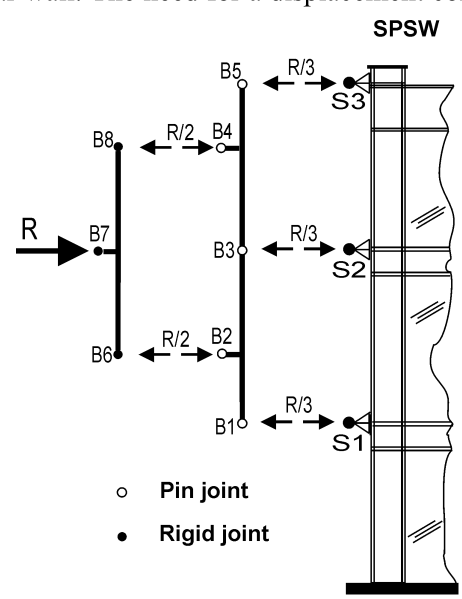

Fig. 2: Loading frame for displacement control of 3SPSW specimen

rotation along the axis of the loading frame element are prevented. Since the selected system is statically determinate, it will not impose any constraint to the shear wall. Therefore, a system of equal horizontal loads can be applied to the shear wall only by controlling the displacement, velocity, or acceleration of node B7. However, with this system only the kinematics of node B7 on the loading frame can be controlled directly, so that, for a parameter other than this node, the control is indirect. For example, to run a cyclic simulation in which the control parameter is first storey drift of the shear wall, a pushover analysis is required to obtain an approximate relationship between node B7 and the first storey drift. This relationship allows a reasonable displacement history at node B7 to yield an approximate drift history for the first panel.

Pushover analysis of three-storey steel plate shear wall

A frequency analysis of the test specimen indicated that the period of the first mode is 3.51 seconds. The total time of the analysis was set at about 50 times the period of the first mode and the initial time increment of the model, which depends on mesh size and material properties (see equation 7), was obtained as 2.322×10^{-4} second. In the first step of the analysis, a gravity load of 540 kN was applied at the top of each column over a loading period of 30 seconds and was kept constant for the remainder of the analysis. The time period of 30 seconds created a quasi-static loading condition as will be shown by a study of the specimen energies.

During the following load step, node B7 was displaced monotonically until the displacement at the first level (node S1 in Fig. 2) reached a value well beyond the displacement at which the specimen reached its ultimate capacity during the test. In order to control the amount of kinetic energy of the specimen, velocity, rather than displacement, was applied smoothly to node B7. Starting at 30 seconds, the velocity history shown in Fig. 3 was applied horizontally to node B7. The shear wall was pushed using a smooth amplitude function so that the velocity and acceleration at the beginning and end of the loading step are zero. Application of the velocity history shown in Fig. 3 resulted in a horizontal displacement of 80 mm at node B7, which created enough drift at the first level to pass the limit point.

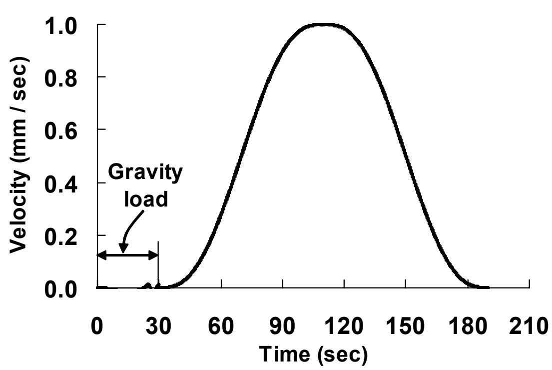

Fig. 3: Horizontal velocity history applied at node B7 for pushover analysis of 3SPSW

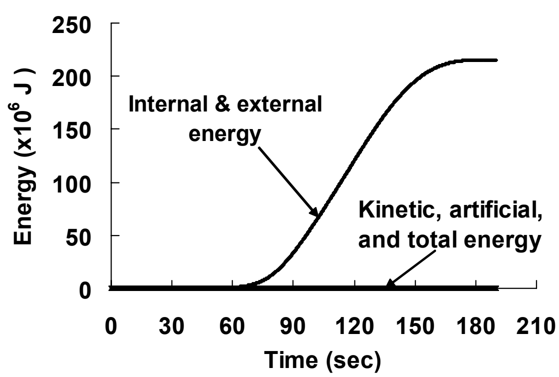

Fig. 4: History of different energies during pushover analysis of 3SPSW

The history of different types of energy developed in the whole system during the pushover analysis is shown in Fig. 4. The internal and external energies are equal and the other forms of energy are negligible relative to internal energy. This indicates that the analysis has been carried out in a quasi-static condition. The artificial energy is also very small compared to the internal energy, which indicates that the hourglass mode has not affected the simulation. The kinetic energy versus time curve presented in Fig. 5 shows that the kinetic energy varies smoothly over time except when the tension field is being developed. When the tension field develops the kinetic energy increases rapidly. This behaviour is characteristic of thin unstiffened steel plate shear walls and it has been observed during the test when the development of the tension field was accompanied by loud reports and rapid out–of–plane deformations in the infill plates [8].

A plot of base shear versus horizontal displacement at the top of the test specimen is presented in Fig. 6. The finite element model is found to predict the stiffness of the shear wall very well but underestimates the strength by about 12%. Since the stiffness of the shear wall is predicted accurately with the finite element model, the lower predicted strength is attributed to the difference in material properties between the finite element model and the three-storey steel plate shear wall test specimen. As explained above, the plastic deformations from the four-storey steel plate shear wall test by Driver *et al.* [3] may have changed the initial yield strength of the infill plate of the first storey of the three-storey specimen. This increase in yield strength is not uniform since the stress field in the infill plate is not uniform over a panel, which makes this factor very difficult to assess and incorporate into the finite element model. Fig. 6 also shows the response of the bare frame, which indicates that the infill plate has significantly increased the stiffness and shear capacity of the frame.

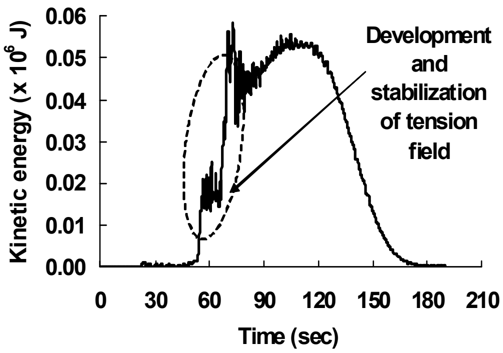

Fig. 5: History of kinematic energy during pushover analysis of three-storey SPSW

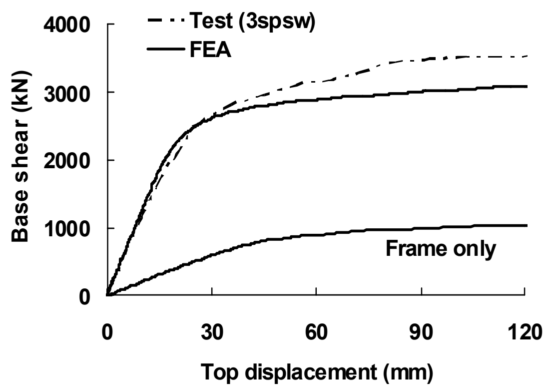

Fig. 6: Base shear vs. top displacement Monotonic FEA compare to envelope of test

Cyclic analysis of three-storey steel plate shear wall

A pushover analysis provides an estimate of the stiffness and capacity of a steel plate shear wall as it captures closely the envelope of cyclic response of a system. However, to evaluate the energy dissipation characteristics and the efficiency of a steel plate shear wall under cyclic loading, the finite element model should be able to simulate accurately the cyclic response of the system.

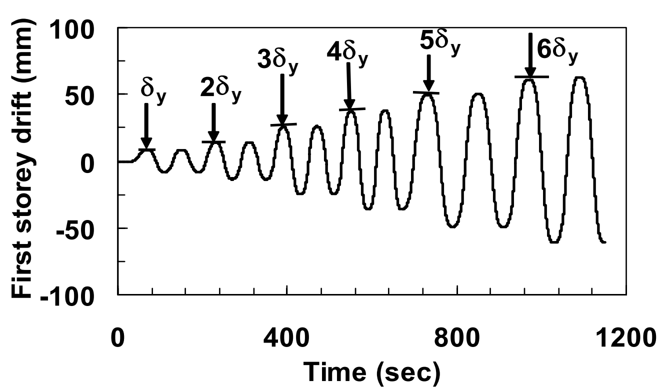

Fig.7: History of drift developed in the first panel of 3SPSW

For simplicity, drift of the first panel was taken as a control parameter to cycle the finite element model. In the first load step the gravity load of 540 kN was applied at the top of each column and was kept constant during the rest of analysis. Based on the relationship between horizontal displacement of node B7 and drift of the first panel (obtained from the pushover analysis of the specimen) the history of displacement at node B7 was developed to create the desirable drift history in the first panel. In the following load steps the shear wall was cycled by increasing drift of the first panel as a multiple of the yield drift. At each displacement level the shear wall was cycled two times in order to develop a stable hysteresis curve. The resulting drift in the first panel as a function of time is presented in Fig. 7. The variation with the time of the different energies was obtained in order to evaluate the inertial effect in the cyclic analysis. It was found that internal and external energies are similar and the kinetic and artificial energies are negligible during the cyclic loading, which indicates that the load model simulated a quasi-static condition.

The hysteresis loops generated from the base shear vs. first storey drift obtained from the finite element analysis and the test is presented in Fig. 8. Good agreement between the test results and the predicted behaviour is observed. The finite element analysis predicts both the initial stiffness and the point of significant yielding accurately. The pinching of the hysteresis curves, which is an important feature of unstiffened steel plate shear wall behaviour, is captured reasonably well by the finite element model. During the early reloading phase, after load reversal, a significant reduction of stiffness occurs after a load reversal. This reduction of stiffness remains until redevelopment of the tension field in the infill plate.

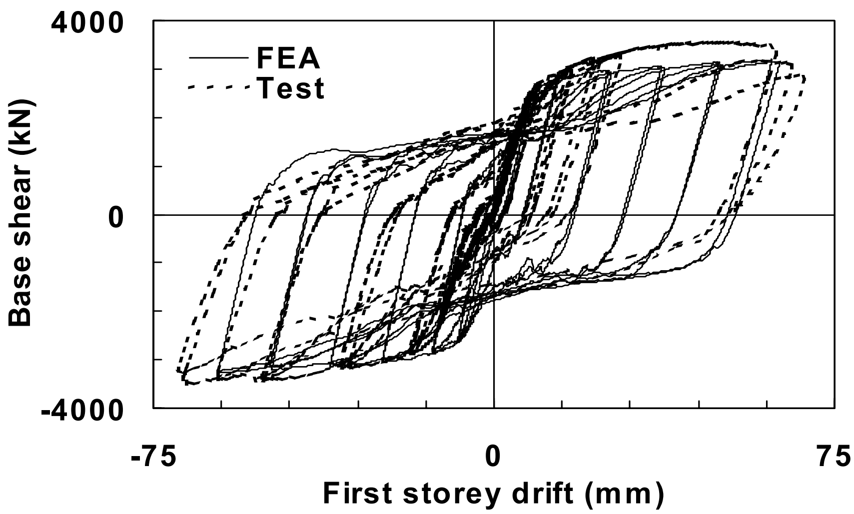

Fig. 8: Finite element hysteresis loops vs. test results (panel 1)

The deformed configuration of the shear wall at three different stages of loading is shown in Fig. 9. Fig. 9a shows the model at full development of the tension field during loading in the east to west direction. Fig. 9b shows the model at an early stage of the redevelopment of the tension field.Fig. 9c shows the deformed shape at full development of the tension field during loading of the shear wall in the opposite direction. The deformed shape obtained from the finite element analysis was very similar to the observed shape during the test. Both show the same configuration and number of buckle waves in the infill plates.

Energy dissipation

The ability of a structural system to dissipate energy is one of the key parameters for evaluating the performance of a system in a severe earthquake. A common approach used to account for inelastic seismic performance of a structural system is to employ a seismic force reduction factor. This factor reduces the elastic spectral demands to a design level that would be encountered if a system possesses significant inelastic behaviour. Structural systems that can effectively dissipate energy are permitted a larger reduction

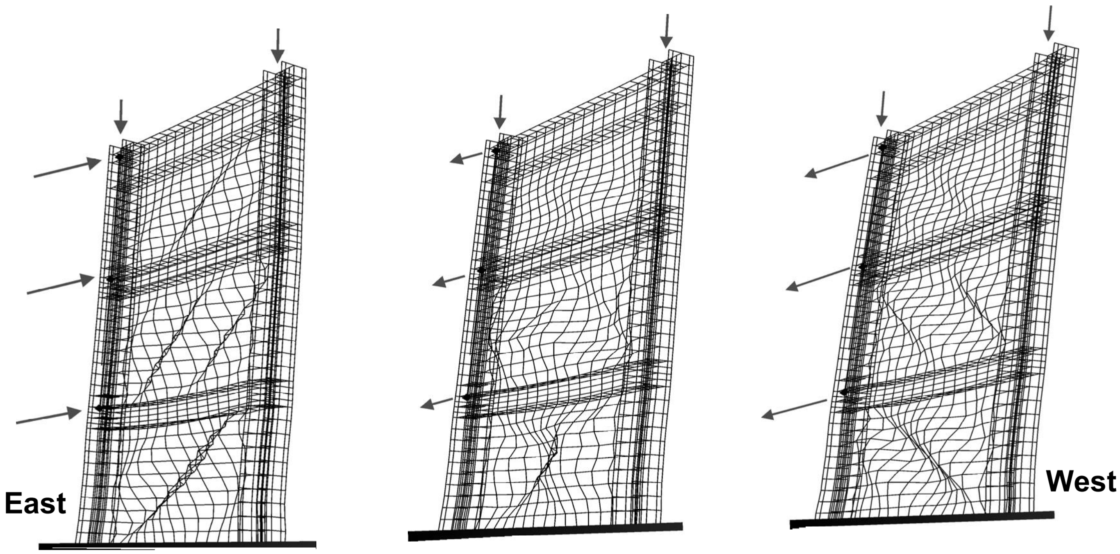

(a) Full development of tension field during loading of the wall in the east to west direction.
(b) At early stage of the redevelopment of the tension field.
(c) At full re-development of tension field during loading of the shear wall in the opposite direction.

Fig. 9: Deformed configuration of three-storey steel plate shear wall

factor. The National Building Code of Canada (NBCC, 1995) introduces a force modification factor, R, to account for inelasticity in the response of a system. The energy dissipation ability of a system is a key parameter used to establish the value for this factor. The area enclosed by hysteresis loops generated during a specific load or displacement history is used as a measure of the energy dissipated by the system.

In order to compare the energy dissipation ability of the finite element model with that of the test specimen, hysteresis loops that have reached a stable behaviour were used. Because the behaviour of the three-storey steel plate shear wall specimen during the test was not symmetrical [8], an unsymmetrical cycle of the test was assumed to be equivalent to a symmetrical cycle with the drift level taken as the average drift from the two excursions.

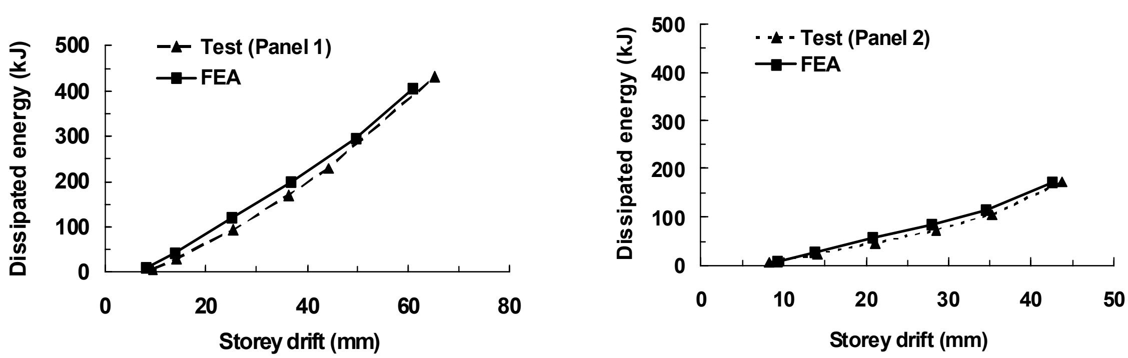

(a) Panel 1 **(b) Panel 2**

Fig. 10: Energy dissipation as a function of drift

The amount of energy dissipated by the first and second panels is plotted against the drift level obtained from the finite element analysis and compared with the test results in Fig. 10. There is excellent agreement between the test and the finite element analysis. At a drift-to-storey height value of 1% the test-to-predicted energy dissipation in panels 1 and 2 is 0.75 and 0.85, respectively. The test-to-predicted energy dissipation at a drift level of 2% is 0.85 and 0.90 for panels 1 and 2, respectively.

SUMMARY AND CONCLUSIONS

A finite element model based on explicit dynamic formulation was developed for the analysis of steel plate shear walls. Material and geometric nonlinearity, and the initial imperfections of the infill plates were included in the model. A kinematic hardening material model subroutine was implemented in order to simulate the Bauschinger effect in the cyclic analysis of the shear wall.

The finite element model was used to simulate the monotonic and cyclic response of a three-storey test specimen. Since the solution strategy in the explicit formulation is not an iterative process, the analysis was completed without any numerical difficulty. In general, excellent agreement was observed between the test results and the finite element analysis. The stiffness of the three-storey steel plate shear wall was predicted accurately, but the predicted capacity was 12% lower than the measured capacity during the test. In general, the hysteresis loops generated by the finite element model were in good agreement with those generated during the test. The pinching effect observed in the physical tests was also captured in the finite element analysis, although to a slightly lesser extent than observed in the physical tests. These results demonstrate the validity and the effectiveness of the developed finite element model of unstiffened steel plate shear walls.

ACKNOWLEDGEMENTS

The research project was funded by the Steel Structure Education Foundation and the Natural Sciences and Engineering Research Council of Canada. Financial support in the form of scholarship was also provided to the first author by the Ministry of Culture and Higher Education of Iran.

REFERENCES

1. Driver, R.G., Kulak, G.L., Kennedy, D.J.L., and, Elwi, A.E., 1998b, “FE and Simplified Models of Steel Plate Shear Wall.” Journal of Structural Engineering, ASCE Vol. 124, No. 2, February, pp. 121-130.
2. Rezai, M., 1999, “Seismic Behaviour of Steel Plate Shear Walls by Shake Table Testing.” PhD Dissertation, Department of Civil Engineering, University of British Columbia, Vancouver, Canada
3. Driver, R.G., Kulak, G.L., Kennedy, D.J.L., and, Elwi, A.E., 1998a, “Cyclic Test of a Four-Story Steel Plate Shear Wall.” Journal of Structural Engineering, ASCE Vol. 124, No. 2, February, pp. 112-120.
4. Canadian Standard Associations, CSA-S16-01, 2001,”Limit States Design of Steel Structures.” Toronto, Ontario
5. Thorburn, L.J., Kulak, G.L., and Montgomery, C.J., 1983, “Analysis of Steel Plate Shear Walls.” Structural Engineering Report No. 107, Department of Civil Engineering, University of Alberta, Edmonton, Canada
6. Bathe, K. J., 1996, “Finite Element Procedures.” Prentice-Hall, Englewood Cliffs, NJ
7. Riks, E., 1979, “An Incremental Approach to the Solution of Snapping and Buckling Problems.” International Journal of Solids and Structures, Vol. 15, No. 7, pp. 529-551.

8. Behbahanifard, M.R., Grondin, G.Y., Elwi, A.E., 2003, “Experimental and Numerical Investigation of Steel Plate Shear Walls” Structural Engineering Report No. 254, Department of Civil and Environmental Engineering, University of Alberta, Edmonton, Canada
9. Benson, D. J., 1992, “Computational Methods in Lagrangian and Eulerian Hydrocodes.” Computer Methods in Applied Mechanics and Engineering, Vol. 99, pp. 235-394.
10. Hibbitt, Karlsson, & Sorenson, Inc., (HKS), 2001, “ABAQUS/Explicit User’s Manual.” version 6.2, Hibbitt, Karlsson, & Sorenson Inc., Pawtucket, Rhode Island.
11. Applied Technology Council, 1992, “Guidelines for Cyclic Seismic Testing of Components of Steel Structures.” ATC-24, Redwood City, CA